Numerical simulation of transient response of heat transfer from a hot-wire anemometer transducer

K. J. Bullock*, M. A. Ledwich† and J. C. S. Lai*

Both the steady state and transient response of the Nusselt number to variations in Reynolds number over the range 1 to 40 are given by the analysis of a time dependent numerical simulation of a hot-wire anemometer transducer described here. Transducer response can be modelled suitably by considering the system to consist of a phase independent non-linearity followed by a non-linear differential equation whose coefficient (approximate time constant) is Nusselt number dependent. Errors associated with slip flow and free convection constrain the minimum size of a hot-wire which may be used in calibration anemometry while the wire thermal inertia and, to a lesser extent, the response of the Nusselt number to Reynolds number limits the use of large diameter wires. Thus, although the tendency has been to use finer and finer wires, the basic fluid mechanics suggests that a compromise in the choice of the wire diameter is appropriate. Thus development of even more sophisticated hot-wire anemometer control systems as well as accurate calibration techniques for measurement in flows containing large amplitude high frequency turbulence is required

Keywords: *heat transfer, flow measurement, turbulence, hot wire anemometry, transient response, thermal boundary layer*

Since the work of King[1], the principle of measuring the heat transferred from electrically heated fine wires suspended in a fluid flow has been universally accepted as a method of determining fluid velocity. Hot-wire anemometers have been used extensively for turbulence measurements even though calibration techniques for measuring the dynamic response of the hot-wires have been very limited. The steady state calibration has been assumed to be valid for dynamic measurements and, although the time constant associated with the thermal capacity of the wire has been well known and determined with square wave injection techniques[2], no satisfactory experimental method has been devised to determine the transient response of the Nusselt number to a perturbation in velocity.

Kidron[3] used a klystron to simulate velocity perturbations up to 50 kHz. Perry and Morrison[4] produced sinusoidal perturbations in the Karman vortex street behind cylinders up to a frequency of 10 kHz. They also demonstrated the difficulty of obtaining derivatives by graphical differentiation of a static calibration curve; the calibration constant thus obtained for a constant resistance anemometer system is at variance with that obtained from a dynamic calibration technique which involves shaking the wire at low frequencies in a uniform flow. Davis[5] used a shock tube to measure the dynamic response but since the temperature dependence of the wire was not eliminated, this is not a valid method of determining the transient response in isothermal conditions.

Very few theoretical studies of unsteady heat transfer from a heated circular cylinder at low Reynolds numbers have been reported except that of Davies[6] who used an Oseen approximation of the energy equation to estimate the fluctuating heat transfer from a heated cylinder at $Re \ll 1$. Several numerical solutions for unsteady heat transfer from a heated circular cylinder have been reported recently[7-10] for the Reynolds number range $100 \leqslant Re \leqslant 200$. The effects of the presence of free convection have been addressed. However, the results were calculated at such large Reynolds numbers that they could not be applied to analyse the response of normal hot wire operation.

The objective of this study was to determine the response of the Nusselt number to velocity transients normal to the wire by solving the two-dimensional time dependent Navier-Stokes and energy equations numerically for $1 \leqslant Re \leqslant 40$. The simulation not only gives the transient response but may also determine steady state values, buoyancy corrections and errors in measurement due to proximity to boundaries or to other wires, as in X-arrays for the measurement of Reynolds stress. The results obtained are also used to develop an appropriate mathematical model for the response of a hot-wire anemometer system.

* Department of Mechanical Engineering, University of Queensland, St Lucia, Brisbane, Australia 4067
† Paper Works System Incorporated, Sydney, Australia 2000
Received 8 May 1984 and accepted for publication on 3 September 1984

Formulation of the problem

By neglecting the effects of heating of the fluid by viscous dissipation and of radiation from the cylinder, the Navier-Stokes equation for two-dimensional flow of an incompressible fluid with constant viscosity and thermal conductivity past a circular cylinder of negligible thermal inertia can be expressed in the form of the non-dimensional vorticity-transport equation:

$$\frac{D\zeta}{Dt}=\frac{2}{Re}\nabla^2\zeta \tag{1}$$

Body forces and the effects of buoyancy are small at the Reynolds number range (1 to 40) to be investigated.

Introducing a stream function ψ, such that $u=\partial\psi/\partial y$ and $v=-\partial\psi/\partial x$, yields:

$$\nabla^2\psi=-\zeta \tag{2}$$

Eq (2) implies that the rates of change of density of the fluid due to changes in temperature are negligibly small so that the mass-conservation equation reduces to the statement that the velocity field is solenoidal.

The energy equation can be expressed as:

$$\frac{DT}{Dt}=\frac{2}{RePr}\nabla^2 T \tag{3}$$

The flow is assumed to be symmetrical about the cylinder and no-slip boundary conditions at the surface of the cylinder are given by:

$$\begin{aligned} &u=0 \quad v=0 \quad T=1 \quad \text{at } r=1\\ &u=1 \quad v=0 \quad T=0 \quad \text{at } r\rightarrow\infty \end{aligned} \tag{4}$$

Eqs (1)–(3) subject to these boundary conditions were solved for $1\leqslant Re\leqslant 40$ by the numerical technique developed by Apelt and Ledwich[11] for the following cases:

1. Step-change in velocity, with wire temperature held constant
2. Sinusoidal perturbation in velocity impressed on a mean flow at $Re=10$ with wire temperature held constant;
3. Step change in wire surface temperature.

The choice of the Reynolds number range and the types of perturbation are discussed below.

Reynolds number range

The steady state heat loss of an electrically heated fine wire has been extensively investigated experimentally. King's data reduces to:

$$Nu=0.335+0.497\,Re^{\frac{1}{2}} \tag{5}$$

This correlation is in good agreement with that determined by Collis and Williams[12].

The requirement of a small heat capacity to reduce the wire time constant, large length-to-diameter ratios to reduce the significance of end-conduction losses and the small current limits of early constant resistance anemometer systems all explain the present practice of using extremely fine wires. These factors plus the requirement of small length necessary to determine the microscale of turbulence have led many workers to use wires of 2 to 5 μm in diameter. Collis and Williams[12] have shown, however, that at Knudsen number (Kn) in the range of 0.03 to 0.012, there are likely to be significant deviations in the Nusselt to Reynolds number relationship. These Knudsen number values correspond to air velocity measurements at atmospheric pressure for wires with diameters of 2 and 5 μm respectively.

On the other hand it would seem that larger diameter wires increase the free convection loss and reduce the accuracy of the measurement at very small Reynolds numbers. Collis and Williams[12], Hatton *et al*[13] and Van der Hegge Zijnen[14] have shown that free convection effects limit the lowest workable Reynolds number. The work of Collis and Williams[12] gives perhaps the most satisfactory statement of a suitable criterion for accurate measurement, namely:

$$Re>Gr^{1/3} \tag{6}$$

However, this criterion simply eliminates the wire diameter from the inequality and states that the minimum velocity which can be measured without free convection effects is $[g\nu\beta(T_w-T_\infty)]^{1/3}$. Furthermore, the data of

Notation

D	Operator, $\frac{d}{dt}$
d	Wire diameter
g	Acceleration due to gravity
Gr	Grashof number
Kn	Knudsen number
$Nu(\theta)$	Local Nusselt number
Nu	Average Nusselt number
Pr	Prandtl number
Re	Wire Reynolds number, Ud/ν
R	Wire radius
r'	Radial distance
r	Non-dimensional radial distance, r'/R
T'	Temperature
T	$(T'-T_\infty)/(T_w-T_\infty)$
T_∞	Ambient temperature
T_w	Surface temperature of wire
t'	Time
t	Non-dimensional time, $t'U/R$
U_τ	Shear velocity
U	Velocity of approach stream
u'	Streamwise velocity
u	Non-dimensional streamwise velocity, u'/U
v'	Transverse velocity
v	Non-dimensional transverse velocity, v'/U
x	Streamwise distance
y	Transverse distance
y^+	Non-dimensional transverse distance, yU_τ/ν
β	Coefficient of thermal expansion
δ_t	Thermal boundary layer thickness
ζ	Vorticity
θ	Cylinder angle from forward stagnation point
ν	Kinematic viscosity
τ'	Time constant
τ	Non-dimensional time constant
ψ	Non-dimensional stream function

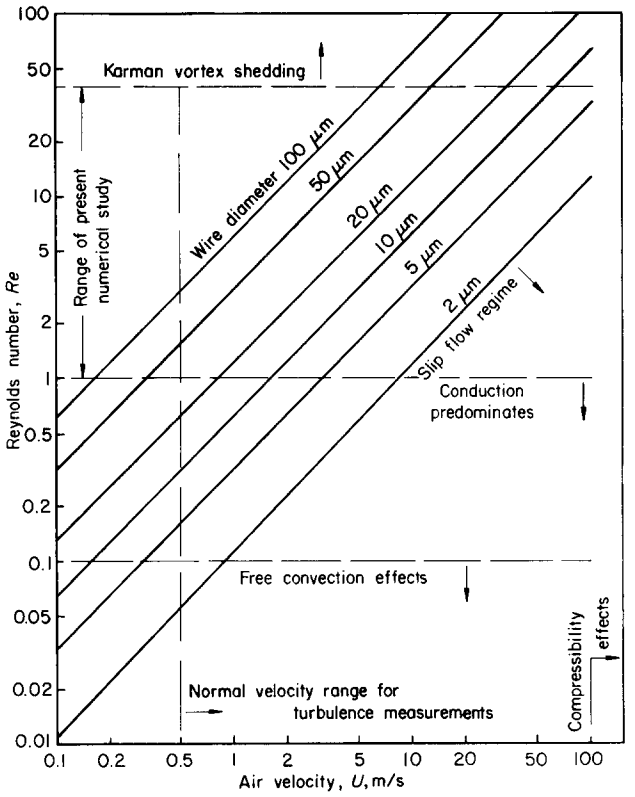

Fig 1 Wire Reynolds number against air velocity showing a suggested operating range

Collis and Williams[12] appear to give a smaller lower limit on Reynolds number than that of Hatton *et al*[13] and Van der Hegge Zijnen[14]. For example, their data would suggest that a 9 μm diameter wire operating over the whole temperature range could be suitable for $Re > 0.03$. However the correlations given in Hatton *et al*[13] and Van der Hegge Zijnen[14], although differing in magnitude of the actual Nusselt number, do agree that below $Re = 0.1$ there is a significant contribution to the combined convection. Thus $Re = 0.1$ has been assumed as a satisfactory lower limit for accurate anemometer measurements. This, and other constraints are shown in Fig 1 for the range of Reynolds number used in subsonic, atmospheric pressure, hot-wire anemometer measurements of air velocity. Since the buoyancy terms were neglected in the numerical study, it was felt that solutions would only be valid for Reynolds numbers an order of magnitude greater than the limit on free convection effects. The lower limit for the numerical solutions, $Re = 1$, also marks the upper limit of the regime where conduction is significant.

Although numerical solutions for the flow past a cylinder above the Karman vortex shedding Reynolds number of 44 have been obtained[7-10,15,16], the presence of eddy shedding means that the contribution of the cylinder wake to the overall Nusselt number might be proportionately more than in the steady flow situation. The experimental work of Collis and Williams[12] shows a marked increase in Nusselt number for Reynolds numbers greater than 40 and a departure from a power law relationship. The Nusselt number might also vary slightly at the eddy shedding frequency which would add to the complications of calculating time constants for step inputs of velocity. Since all subsonic flows can be measured with an upper constraint of $Re = 40$ (Fig 1), this value of the Reynolds number has been chosen as the upper limit for the simulation to avoid complications arising from the vortex shedding phenomenon.

Types of perturbations

Step change in velocity

A step is of course an unrealistic velocity perturbation except perhaps in a shock tube but there the velocity jumps are enormous and accompanied by large temperature changes as well. A ramp function would have been as useful to identify a single time constant system. However, the results are more difficult to interpret if the system consists of multiple time constants. The step function response gives adequate information for the identification of the system and enables the boundary condition be changed only at zero time. Thus the boundary conditions are constant both before and after the transient and this produces a slight advantage in the computational procedure as discussed more fully by Apelt and Ledwich[11]. A 50% size in the perturbation was chosen to:

ensure that the evaluation of the time constant was not affected by the computational accuracy;
give additional data points on the steady state relationships;
check the basic mathematical model for the response of the hot-wire anemometer.

Three initial Reynolds numbers, namely 1, 10 and 26.67, were chosen to give final values of 1.5, 15 and 40 respectively.

Sinusoidal perturbation in velocity

A small, 10% change, about $Re = 10$ (the midpoint of operation of hot-wires) at a frequency calculated to be the corner frequency from the above transient response, was chosen to substantiate the time constants measured by step function response.

Step change in wire surface temperature

The common practice of using a square wave injection technique for the determination of the wire time constant relies on the fact that the response of the heat transfer to a wire surface temperature perturbation is much faster than that of either a constant current or constant resistance hot-wire anemometer system.

A step function in the surface temperature was easily incorporated into the numerical programme and represents the rather unrealistic case of an impulse plus a step function of heat or current into a wire of negligible mass or specific heat. It might be thought that a ramp in the wire surface temperature would be a more suitable boundary condition which would correspond to a step and a ramp in wire current. However, this would only identify the time constant associated with the mean heat transfer coefficient. Alternatively if a decaying exponential was assumed for the history of the wire surface temperature, the details of the short time constants associated with the fluctuations in the surface temperature would not be detected.

The mathematical model and to a lesser extent the physics of the heat transfer indicates that Nusselt number will be very large for a step change in the temperature of the wire. This indicates that the system will differentiate the input and then, following the transient decay, return

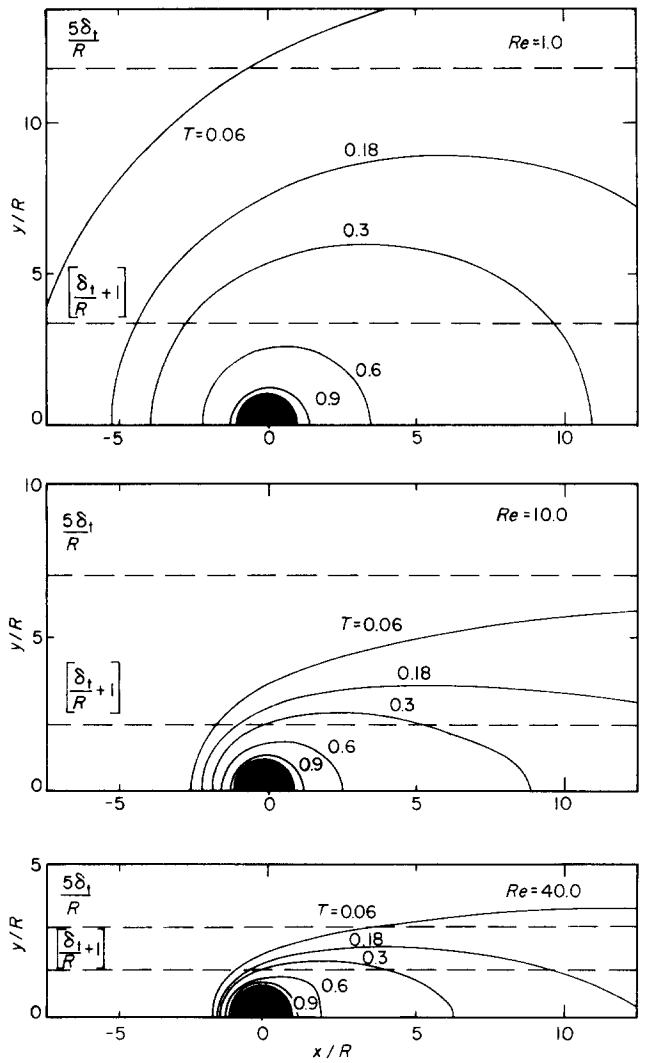

Fig 2 Air temperature profiles in the vicinity of a hot-wire element

the output to the initial Nusselt number. The size of the jump (100%) is immaterial in the constant property system analysis.

Steady state solution results

Temperature profiles

The isotherms for the three Reynolds numbers (1, 10 and 40) are presented in Fig 2. At high Reynolds numbers the thermal boundary layer is thin as is the width of the thermal wake.

Walker and Bullock[17] have verified experimentally the wake thickness relationship of Hinze[18], namely that the standard deviation of the Gaussian distributed wake thickness behind a line source of heat is proportional to $[x/U]^{1/2}$. The temperature profiles of Fig 2 show the tendency towards the normal distribution although the downstream boundary condition and the finite grid limit its full development.

As the flow speed is decreased, the temperature profiles tend towards a symmetrical solution about $x/R=0$ and in the absence of free convection at Reynolds numbers of the order of 0.1, the profiles would approach the pure conduction case.

Grant and Kronauer[19], in discussing velocity measurements close to a boundary, stated that the wire thermal boundary layer thickness (δ_t) is approximately equal to d/Nu. The thermal boundary layer obviously increases as Reynolds number decreases and a check on δ_t given by Grant and Kronauer[19] can be made by plotting the ordinate $[\delta_t/R+1]$ on those contour plots of Fig 2. The complete results show that for the Reynolds numbers greater than 10 this ordinate is a tangent to the 0.4 isotherm. For the Reynolds numbers 5 and 1 this criterion cuts progressively into the higher isotherms.

Grant and Kronauer[19] also stated that hot-wires can be used as close as $5\delta_t$ from a boundary. This distance is also marked on the temperature profiles of Fig 2. As the ordinate $5\delta_t/R$ cuts into the isotherm 0.06 for $Re=1$ but not for $Re=10$, this criterion would seem to be applicable for $Re>10$ but less valid for $Re<1$. In fact, the results for $Re=5$ (not shown here) indicate that this criterion is valid for $Re>5$. Thus, until accurate solutions of the profiles are obtained close to a boundary and with free convection terms included, it seems prudent to limit measurements to $Re>1$ close to a boundary and wall distances greater than $15R$ for $Re<5$. To take a specific example, for a boundary flow of $U_\tau=1$ m/s, $y^+=3$ occurs at $9d$ for a 5 μm diameter wire at $Re=1$. Nevertheless, it must be pointed out that wires which are used at distances from the surface one order of magnitude greater than the wire diameter may give inaccurate results because of the excessive spanwise length of the wire and the non-linear variation of temperature along its length: the relative intensity near the wall is large whereas typical eddy sizes are of the order of the distance from the surface and therefore much less than typical wire length.

Local Nusselt number around the cylinder

The local Nusselt number around a cylinder is defined as:

$$Nu(\theta)=-2\left(\frac{\partial T}{\partial r}\right)_{r=1} \tag{7}$$

and the average Nusselt number as:

$$Nu=\frac{1}{\pi}\int_0^{\pi} Nu(\theta)\,d\theta \tag{8}$$

The steady state local Nusselt number $Nu(\theta)$ is shown for the Reynolds numbers 1 to 40 in Fig 3 and illustrates the fact that, at $Re=1$ there is very little variation in the radial gradient of the temperature profile around the cylinder; Fig 2 also confirms this. As the Reynolds number increases, there is a large increase in the Nusselt number at the forward stagnation point but little increase in the region for $\theta>120°$. This shows that the contribution of the tail to heat loss is not very important. At $Re=40$ there appears to be an increase in the local Nusselt number from $\theta=120°$ to $\theta=180°$ and this agrees with the approach of the eddy shedding at $Re=44$. It is well known that in turbulent flow around the cylinder (see for example Knudsen and Katz[20]) there is a minimum in the local $Nu(\theta)$ at the separation point which normally occurs at $\theta>80°$. This result also appears in the work of Eckert and Soehngen[21] where the experimental result for $Re=23$ is shown in Fig 3. Excellent agreement exists over the range of $\theta=0$ to 100°. These workers used cylinders with diameters large when compared with those used for hot-wire work, that is, 12.7 to 38.1 mm and an interferometer

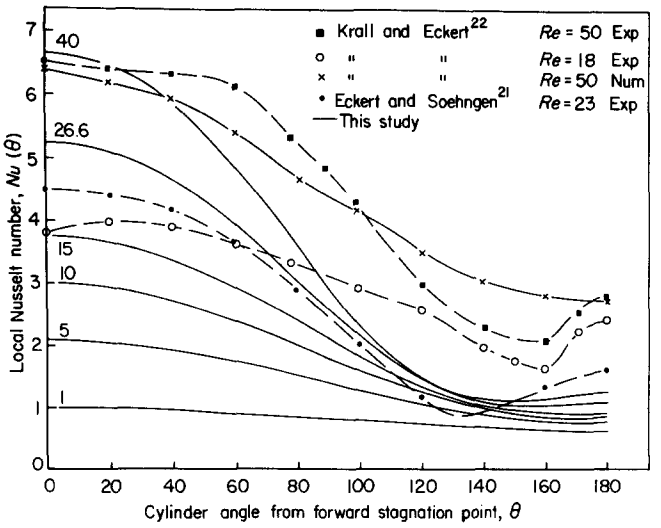

Fig 3 Local Nusselt number against angular position for Reynolds numbers 1 to 40

to measure the temperature distribution. However they relied on decelerating flow for their low Reynolds number measurements and this could account for the discrepancy between their results and our numerical study. Krall and Eckert's numerical solution[22] for slip flow and constant heat flux at a Reynolds number of 50 is also shown in Fig 3. Both slip flow and constant heat flux reduce the heat transfer at the forward stagnation point and increase it at the rear stagnation point. Their experimental results for $Re=18$ and 50 are at variance with the present numerical study because of the variation in the boundary condition, namely slip flow and constant heat flux. However, in addition, their experimental results were corrected for a circumferential conduction heat loss of up to 25% and this inaccuracy has presumably produced the rather anomalous situation of a non-maximum heat transfer at the forward stagnation point.

Average Nusselt number

The local Nusselt numbers of Fig 3 when integrated from 0 to π give the average Nusselt number for each Reynolds number. Fig 4 shows that there is a near perfect correlation with $Re^{1/2}$, namely:

$$Nu=0.3702+0.4847Re^{1/2} \tag{10}$$

This compares well with King's relationship given in Eq (5). The data of Collis and Williams[12] in Fig 4 agree remarkably well with the numerical results for the overheat ratio $T_w/T_\infty=2.0$. However, the data for the small $T_w/T_\infty=1.1$ are significantly lower than the constant property solutions of the present study with which they would be expected to agree. Collis and Williams[12] preferred the correlation:

$$Nu=0.24+0.56Re^{0.45} \tag{11}$$

for small overheat ratios.

In practice, the difference between a 0.5 power curve fit and a 0.45 power curve fit can be significant in evaluating the slope, as demonstrated by Perry and Morrison[4].

Velocity transient results

Response of Nusselt number to step input of velocity

The time response of the Nusselt number for 50% step changes in the velocity from Reynolds numbers 1, 10 and 26.66 are given in Fig 5. The response at the higher Reynolds numbers appears similar to that of a single time constant linear system. As is to be expected, the time to reach 0.63 of the increment to the final value, ie the time constant, decreases with increasing Reynolds number. For the case of $Re=1$, many more computational time steps would have been required for the Nusselt number to reach the final state. The time constant at $Re=26.6$ appears to be $0.8\,d/U$. At $Re=10$, this time is increased by 50% while at $Re=1$ it is approximately five times this basic time. An examination of the extent of the steady state temperature profiles of Fig 2 or of $Nu(\theta)$ of Fig 3 shows that this result is not unexpected.

Response of the Nusselt number to a sinusoidal input

To reduce the uncertainty regarding the Reynolds number for which the time constants τ determined from Fig 5 are applicable, a small sinusoidal perturbation of velocity of 10% at a Reynolds number of 10 was chosen as the input to the simulation. An estimate of τ at $Re=10$ is 2.3 so that $\omega=2.3^{-1}$ was chosen for the input frequency. Both the input and the output of the simulation are given in Fig 6. The average magnitude of the output is 0.703 while the phase shift is 43°. Had the time constant τ been chosen exactly, and presuming that the system can be linearized, the magnitude ratio and phase would be 0.707 and 45° respectively.

A data fit to magnitude and to phase gives $\tau=2.3$ and 2.1 respectively. A compromise of $\tau=2.2$ is acceptable and fits the data of Fig 8 which is derived from the step input results.

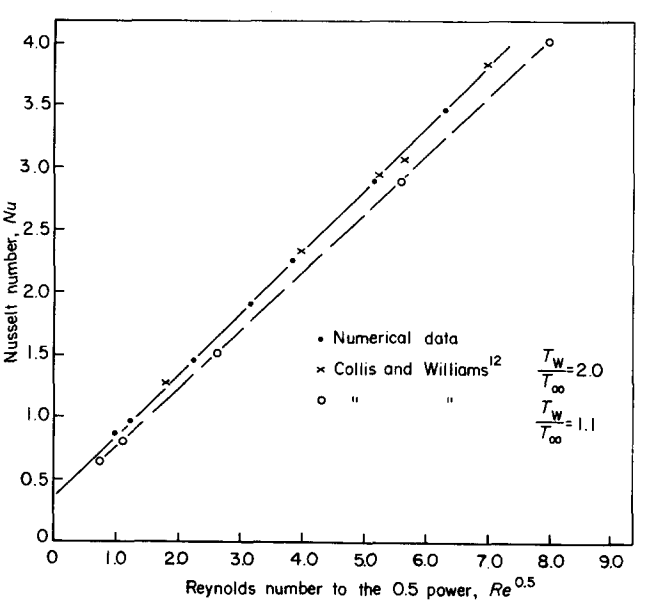

Fig 4 Nusselt number against Reynolds number to the 0.5 power

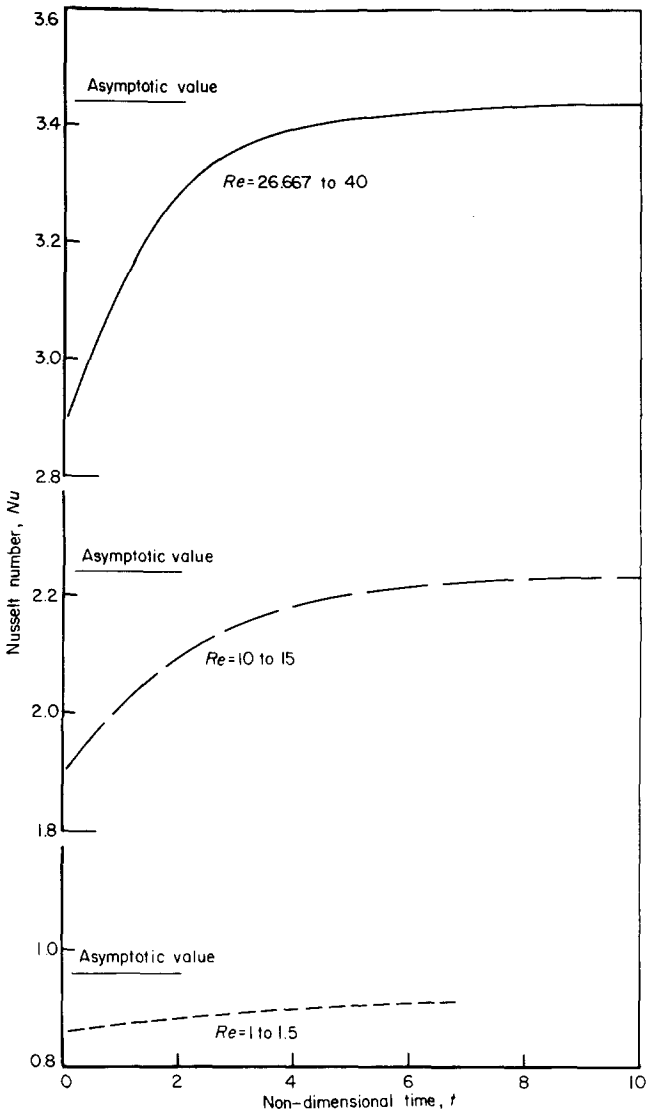

Fig 5 Nusselt number against non-dimensional time for a step input of velocity

Surface temperature transient results

The responses of the simulation to a step change in the surface temperature from $T=1$ to $T=2$ for the Reynolds numbers 5 and 40 are shown in Fig 7. The solution for $Re=1$ although giving similar trends, oscillated violently at a frequency of 31 rad/t and a damping ratio of 0.065.

As is to be expected, the Nusselt number rises immediately to very large values and then decays. The impulse response is due to the fact that the surface temperature has been changed instantaneously while the isotherms surrounding the cylinder in the air stream remain as for the previous boundary condition. The decay is not a simple exponential but is due to the distributed nature of the isotherms which all reach equilibrium with different time constants. The best fit to the exponential data at a Reynolds number of 5 is:

$$Nu(t)-Nu_{\text{final}}=7.06e^{-27.45t}+1.85e^{-2t}+0.245e^{-0.184t} \quad (11)$$

This expression fits the 40 data points over the range $t=0.025$ to 11 with a maximum error of 1% of the value at $t=0.025$. Thus the time constants associated with the response to a temperature transient are 0.036, 0.5 and 5.4 on a non-dimensional scale of time. The residues associated with these terms show that, for the majority of the transient after $t=1$, the second time constant is probably the predominant one. Fig 8 gives the time constant for a velocity transient at this Reynolds number as equal to 3. It is thus not unexpected that the response to temperature disturbances of the wire surface is on the whole faster than the response to velocity since the majority of the thermal resistance occurs in the very thin layer in the region of the forward stagnation zone.

Bradbury and Castro[23] used a pulsed current superimposed on a mean current to obtain wire time constants for wires of 5.3 μm, 7.87 μm and 10.9 μm in diameter and for flow velocities up to 12 m/s. The non-dimensional time constant τ calculated from their data for $Re=5$ is 2.9, 3.4 and 3.0×10^3 respectively. These results demonstrate that the time constants associated with the

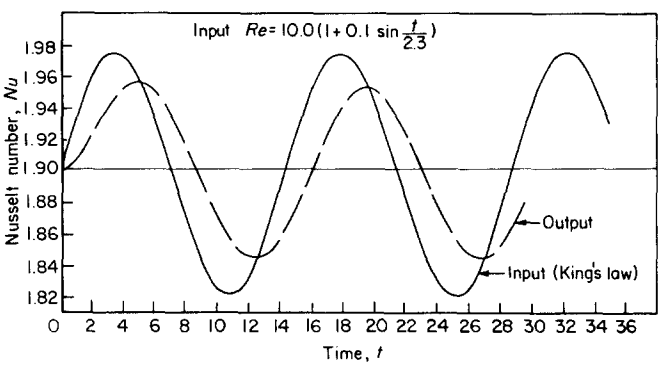

Fig 6 Nusselt number against non-dimensional time for a sinusoidal perturbation of velocity

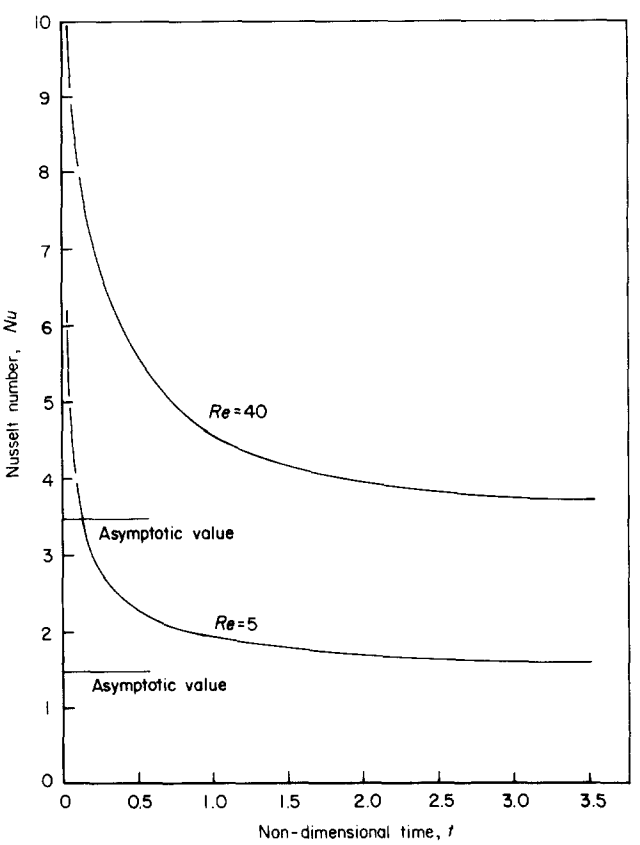

Fig 7 Nusselt number against non-dimensional time for a step change in cylinder surface temperature

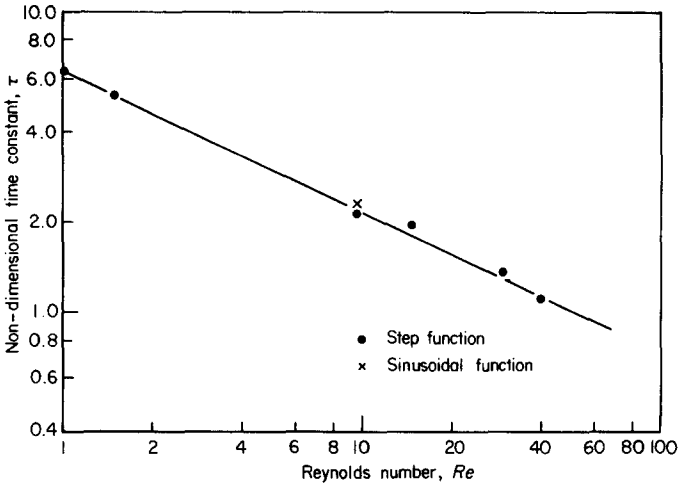

Fig 8 Small perturbation non-dimensional time constant against Reynolds number

mean heat transfer coefficient and the heat capacity of the wire is three orders of magnitude more significant than the time constant associated with wire surface temperature fluctuations in a steady stream as calculated by our numerical techniques.

It is presumed that the response to an ambient temperature change would be similar to that for velocity since the vorticity and temperature equations are identical in form but with different boundary conditions.

Mathematical models of a hot-wire transducer and non-dimensional time constants

Three simple models of the non-linear hot-wire anemometer transducer (Fig 9) are possible:

(a) a non-linearity precedes the dynamics of the system whose coefficients are Reynolds number dependent;
(b) the non-linearity follows the dynamics of the system which is Reynolds number dependent;
(c) the non-linearity precedes the dynamics of the system whose coefficients are Nusselt number dependent.

The computational results are easily examined in terms of the first model and a numerical technique was used to minimize the variance between the data points and dynamic models consisting of first, second and third order systems with and without delays of $t=2$ for the second and third approximate time constants. This analysis showed that the first order system gave minimum variance, and that higher order models did not reduce the variance nor the absolute value of the error but readjusted the location of the maximum error. Values of 8, 2.4 and 1.65 were obtained for the approximate time constants for 50% velocity jumps from $Re=1$, 10 and 26.66 respectively.

Since the size of the computational velocity jump is large, being purposely chosen to improve the signal-to-noise ratio, there is considerable doubt about the location of this time constant; for example, does 1.65 apply to $Re=26.6$, to $Re=40$, or somewhere in between? The more realistic Model (c) was then proposed as an analysis of Model (b) showed that this model was less satisfactory than Model (a).

It is realized that, in the true sense of the words, 'time constant' can only apply to time invariant linear systems. The second portion of Model (c), that is, the relationship between $Nu(t)$ and $Nu(\infty)$ can be described only with a non-linear differential equation but the 'time constant' and 'corner frequency' concept to be introduced is applicable for small turbulence measurements when τ is approximately constant.

The preliminary data of Model (a) were used to estimate the time constant in real time for a particular wire as a function of Nusselt number $\tau(Nu)$. Since the first order fit to Model (a) gave the best results, the following differential equation:

$$\frac{dNu(t)}{dt}=\frac{Nu_{final}-Nu(t)}{a-bNu(t)} \tag{12}$$

was solved for the three velocity jumps and an optimization of the coefficients a and b of the approximation to $\tau(Nu)$, that is:

$$\tau(Nu)=a-bNu(t) \tag{13}$$

was carried out for the 50% variation in Re under analysis. The results are given in Table 1 and plotted in Fig 8. The time constant obtained from the sinusoidal perturbation is also included in Fig 8 and fits the correlation obtained from the transient response. A regression analysis of the non-dimensional time constant gave:

$$\tau=6.37Re^{-0.471} \tag{14}$$

Corner frequencies of hot-wire transducers

The corner frequency (or 3 dB point) of a hot-wire transducer in air can now be calculated using the data of Table 1 or Fig 8. The corner frequency f_c is a strong function of velocity for a wire of a particular diameter and is only applicable to small turbulence levels $\simeq 10\%$.

$$f_c=\frac{U}{\pi d\tau} \tag{15}$$

Eqs (14) and (15) combine to give:

$$f_c=9.123\frac{U^{1.471}}{d^{0.529}} \tag{16}$$

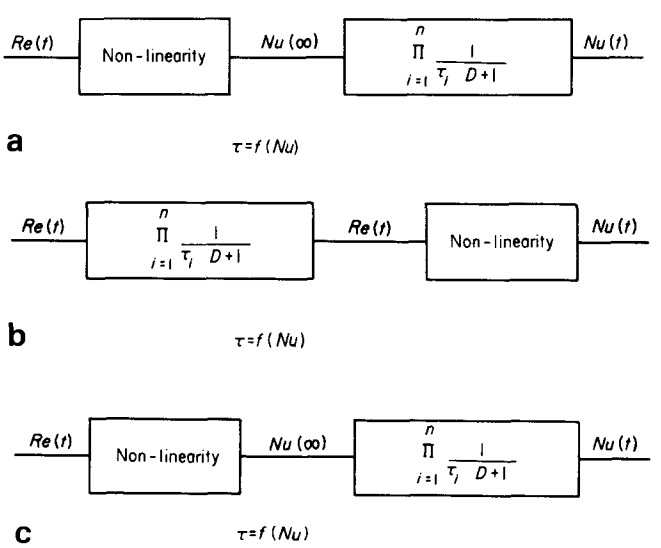

Fig 9 Mathematical models of a hot-wire transducer

Table 1 Estimates of real time constants for a 20 μm diameter wire and the non-dimensional time constant

Re	*Nu*	τ', μs	$\tau\left[\frac{t'U}{R}\right]$	Maximum error	*a*	*b*
1	0.86046	80.00	6.4	0.34%	367.8	339.5
1.5	0.96690	44.40	5.2			
10	1.89895	2.39	2.1	0.49%	8.14	3.03
15	2.24227	1.58	1.9			
26.66	2.87146	0.61	1.34	0.63%	1.967	0.473
40	3.44234	0.34	1.10			

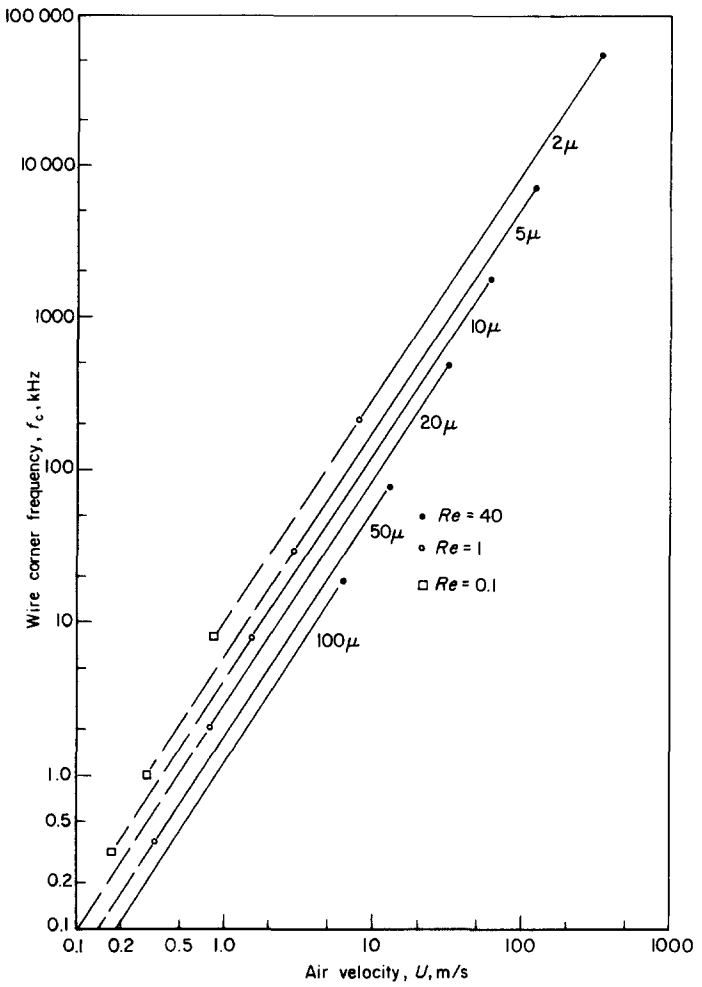

Fig 10 Small perturbation wire corner frequency against air velocity

The curves of Fig 10 are drawn for the maximum range of wire diameter useful for hot-wires, ie 2 to 100 μm and for the Reynolds numbers 0.1 to 40. The solid lines are drawn for the range of Reynolds number of the present numerical study and are extrapolated to a limit for Reynolds number = 0.1 on the presumption that the above correlation for τ extends to this lower Reynolds number which is very often in the operating range of turbulence measurements (Fig 1). A 10 μm diameter wire covers the velocity range 1.5–60 m/s with corner frequencies extending from 8 kHz to 17 MHz. This wire also satisfies the Knudsen number, Karman vortex shedding and buoyancy constraints of Fig 1 and is therefore an acceptable compromise for most subsonic anemometry. However, using the Bradbury and Castro[23] data, this wire would have a corner frequency of only 80 Hz at a velocity of 10 m/s. Thus, although the velocity to heat transfer transient response is adequate, sophisticated compensation systems have to be used to extend the system operating frequency up to a usable range of say 10 to 20 kHz.

In addition, the difficulty of measuring high frequency perturbations at low velocities of the order of 0.3 m/s is illustrated in Fig 10. The corner frequency of 100 μm diameter wire is only 200 Hz and even if a 5 μm wire were used which is on the buoyancy limit (Fig 1), and the relevant curve could be extrapolated, the frequency response would be at best 1 kHz. Furtunately the spectra of turbulence at $y^+ = 1$ for $U_\tau = 0.3$ m/s are less than 1 kHz.

Conclusion

The numerical simulation presented here has verified the steady state relationships of King[1] and Collis and Williams[12]. The work also substantiates the thermal boundary layer criterion proposed by Grant and Kronauer[19] for $Re > 5$ and suggests that free convection is not generally a restriction. In addition it has shown that for the majority of hot-wire anemometer applications measuring small turbulence levels, the transient response of the heat transfer to velocity perturbations has a relatively unimportant effect on spectral measurements.

Small wires of the order of 2 microns in diameter are to be preferred both for this transfer function and for that associated with the heat capacity of the wire and the mean heat transfer coefficient. However, as shown in Fig 1, this small diameter wire is on the slip flow regime and free convection effects occur at velocities which exist in the wall region of normal boundary layer flows. The errors produced by these two phenomena can only be eliminated by carrying out an accurate and complete calibration. On the other hand, it appears that a wire of diameter 10 μm satisfies all the constraints as regards the basic fluid mechanics of the transducer. However, a wire of this size is unfortunately subject to a slow electrical transient response time due to its thermal inertia. The development of sophisticated instruments will reduce the difficulty of measuring high frequency components with wires of this size and may improve the overall accuracy of the hot-wire anemometer system.

It has also been shown that the best mathematical

model of the transducer uses a non-linear (King's law) relation followed by a high frequency response portion consisting of a Nusselt number dependent first order system. Thus, with an elaborate control system incorporated in a hot-wire anemometer instrument whose frequency response is independent of the magnitude of the heat loss, an adequate open loop compensation may be used to measure accurately large scale turbulence fluctuations normal to a hot-wire.

Acknowledgements

The authors gratefully acknowledge the financial support received from the University of Queensland Research Funds and from the Australian Research Grants Committee. In addition, the Australian Institute of Nuclear Science provided access to the Australian Atomic Energy Commission's computer. Professor C. J. Apelt of the Department of Civil Engineering, University of Queensland, suggested the technique of numerical analysis and supervised this portion of the work. His contribution is much appreciated.

References

1. **King L. V.** On the convection of heat from small cylinders in a stream of fluid: determination of the convection constant of small platinum wires with applications to hot-wire anemometry. *Phil. Trans. A. 1914*, **214**, *373–432*
2. **Kronauer R. E.** Survey of hot-wire theory and techniques. *Pratt and Whitney Research Report, 137, Harvard University, Dec. 1953*
3. **Kidron I.** Measurement of the transfer function of hot-wire and hot-film turbulence transducers. *IEEE Trans. on Instr. and Meas. 1966*, **IM-15** *(3), 76–81*
4. **Perry A. E. and Morrison G. L.** Static and dynamic calibration of constant temperature hot-wire systems. *J. Fluid Mech. 1971*, **47**, *765–777*
5. **Davis M. R.** The dynamic response of constant resistance anemometers. *J. Phys. E, Sci. Instr. 1970*, **3**, *15–20*
6. **Davies H. G.** Fluctuating heat transfer from hot wires in low Reynolds number flow, *J. Fluid Mech. 1976*, **73**, *49–51*
7. **Jain P. C. and Goel B. S.** A numerical study of unsteady laminar forced convection from a circular cylinder, *ASME J. Heat Transfer 1976*, **98**, *303–307*
8. **Sano T.** Short-time solution for unsteady forced convection heat transfer from an impulsively started circular cylinder. *Int. J. Heat Mass Transfer, 1978*, **21**, *1505–1516*
9. **Jain P. C. and Lohar B. L.** Unsteady mixed convection heat transfer from a horizontal circular cylinder. *ASME J. Heat Transfer, 1979*, **101**, *126–131*
10. **Tseng W. F. and Lin S. P.** Transient heat transfer from a wire in a violently fluctuating environment. *Int. J. Heat Mass Transfer, 1983*, **26**, *1695–1705*
11. **Apelt C. J. and Ledwich M. A.** Heat transfer in transient and unsteady flows past a heated circular cylinder in the range $1 \leqslant R \leqslant 40$. *J. Fluid Mech., 1979*, **95**, *761–777*
12. **Collis D. C. and Williams M. J.** Two-dimensional convection from heated wires at low Reynolds numbers, *J. Fluid Mech. 1959*, **6**, *357–384*
13. **Hatton A. R., James D. D. and Swire H. W.** Combined forced and natural convection with low-speed air over horizontal cylinders, *J. Fluid Mech., 1970*, **42**, *17–31*
14. **Van der Hegge Zijnen B. G.** Modified correlation formulae for the heat transfers by natural and by forced convection from horizontal cylinders. *Appl. Sci., Res., Sect. A, 1957*, **6**, *129–140*
15. **Dennis S. C. R. and Chong G. I.** Numerical solutions for steady flow past a circular cylinder at Reynolds numbers up to 100. *J. Fluid Mech., 1970*, **42**, *471–489*
16. **Scala S. M. and Gordon P.** Solution of the time-dependent Navier-Stokes equations for the flow around a circular cylinder, *AIAA Journal, 1968*, **6**, *815–822*
17. **Walker T. B. and Bullock K. J.** Measurement of longitudinal and normal velocity fluctuations by sensing the temperature downstream of a hot wire, *J. Phys. E, Sci. Instrum. 1972*, **5**, *1173–1178*
18. **Hinze J. D.** Turbulence, *McGraw-Hill, New York, 1975*
19. **Grant H. P. and Kronauer R. E.** Fundamentals of hot-wire anemometry. *ASME Symposium on Measurement in Unsteady Flow, 1962*
20. **Knudsen J. G. and Katz D. L.** Fluid dynamics and heat transfer, *McGraw-Hill, New York, 1958*
21. **Eckert E. R. G. and Soehngen E.** Distribution of heat transfer coefficients around circular cylinders in cross flow for Reynolds numbers from 20–500. *Trans. ASME, 1952*, **74**, *343–347*
22. **Krall K. M. and Eckert E. R. G.** Local heat transfer around a circular cylinder at low Reynolds number and in transverse slip flow. *ASME preprint 70-HT/Sept. 1970*
23. **Bradbury L. J. S. and Castro I. P.** Some comments on heat transfer losses for fine wires. *J. Fluid Mech. 1972*, **51**, *pp 487–495*

CALENDAR

10th IMEKO Congress	22–26 April 1985 Prague, Czechoslovakia	10th IMEKO World Congress Secretariat, House of Technology, Gorkeho nam 23, 112 82 Prague 1, Czechoslovakia
Symposium on Transport Phenomena in Rotating Machinery	28 April–3 May 1985 Honolulu, HI, USA	Professor Wen-Jei Yang, Department of Mechanical Engineering and Applied Mechanics, 2150 G.G. Brown Building, University of Michigan, Ann Arbor, MI 48109, USA
Industrial Fluid Flow Computation	22–23 May 1985 Middlesbrough, UK	Dr A. W. Bush, Department of Mathematics and Statistics, Teeside Polytechnic, Borough Road, Middlesbrough, Cleveland TS1 3BA, UK
2nd International Conference on Multiphase Flow	19–21 June 1985 London, UK	Conference Organiser, Multi-Phase Flow, BHRA, The Fluid Engineering Centre, Cranfield, Bedford MK43 0AJ, UK
Turbulence Methods for Computational Fluid Dynamics (course)	19–21 June 1985 London, UK	Dr M. M. Gibson, Mechanical Engineering Department, Imperial College of Science and Technology, Exhibition Road, London SW7 2BX, UK